

## Generation of stimulated Brillouin scattering in a packaged $\text{CaF}_2$ micro-disk resonator with ultra-high-Q factor

YANG Yu<sup>1</sup>, ZHAO Shuai<sup>1</sup>, SHEN Yuan<sup>1</sup>, MENG Ling-Jun<sup>1</sup>, WANG Meng-Yu<sup>2</sup>,  
ZHANG Lei<sup>1</sup>, WANG Ke-Yi<sup>1\*</sup>

1. Department of Precision Machinery and Precision Instrumentation, University of Science and Technology of China, Hefei 230026, China;
2. Key Laboratory of Nondestructive Test of Ministry of Education, Nanchang Hang-kong University, Nanchang 330063, China)

**Abstract:** The whispering gallery mode (WGM) micro-resonator is an ideal platform for investigating the nonlinear light phenomenon. In this article, we achieved up to the fifth-order cascaded stimulated Brillouin scattering (SBS) light in a  $\text{CaF}_2$  micro-disk resonator with an mm-sized 12.6 mm diameter and an ultra-high quality factor ( $Q$  factor)  $1.16 \times 10^8$  at 1550 nm wavelength. We found that there are multi modes of families in our large-scale micro-disk resonator when coupled to an adiabatic tapered fiber, which can easily select resonances matching the SBS frequency shift. This can eliminate the requirement that precisely controls the scale of the resonator to match the free spectral range (FSR) with the Brillouin frequency shift. During our experiment, to solve the environmental fluctuation problem between the micro-disk resonator and tapered fiber, we designed a packaged platform that can steadily seal the resonator and tapered fiber in an  $\text{N}_2$  atmosphere. The generated cascaded Brillouin light and the stable packaged platform can further be used to investigate the multi-wavelength Brillouin laser and Brillouin light-based gyroscope.

**Key words:** whispering gallery mode, packaged whispering gallery mode (WGM) resonator, stimulated Brillouin scattering (SBS), Brillouin laser

**PACS:** 42. 55. Sa, 42. 65. Es, 42. 70. -a

## 基于超高Q值封装 $\text{CaF}_2$ 晶体盘腔的级联受激布里渊散射光产生

杨煜<sup>1</sup>, 赵帅<sup>1</sup>, 沈远<sup>1</sup>, 孟令俊<sup>1</sup>, 王梦宇<sup>2</sup>, 张磊<sup>1</sup>, 王克逸<sup>1\*</sup>

1. 中国科学技术大学精密机械与精密仪器系, 安徽合肥 230026;
2. 南昌航空大学教育部无损检测重点实验室, 江西南昌 330063)

**摘要:** 回音壁模式光学微腔是一种研究非线性光学现象的理想平台。在1550 nm波段下成功实现了在 $\text{CaF}_2$ 晶体微腔中产生五阶级联的受激布里渊散射激光。所用的 $\text{CaF}_2$ 晶体微腔直径为12.6 mm,同时有着超高的品质因子,最高可以达到 $1.16 \times 10^8$ 。实验中发现,当大尺寸晶体腔与绝热的锥形光纤进行耦合时,能够激发出多个谐振模式,保证了能够方便地选择不同的谐振波长来匹配受激布里渊散射频移。可以消除在匹配微腔的自由频谱范围和布里渊频移时对微腔尺寸精准控制的需要。为了解决在微腔和波导耦合时的环境震动影响,还设计了一个可以精密耦合调节的封装平台,可以保证谐振腔和波导稳定的在氮气保护气体氛围中被耦合密封起来。产生的级联布里渊激光和设计出的稳定封装平台可以用于后续的应用开发,例如多波长布里渊激光器产生和基于布里渊激光的陀螺仪研发等。

**关键词:** 回音壁模式;封装微腔;受激布里渊散射

中图分类号:O43 文献标识码:A

Received date: 2021-02-26, revised date: 2021-09-03

收稿日期:2021-02-26,修回日期:2021-09-03

Foundation items: the Fundamental Research Funds for the Central Universities (WK5290000001), the Natural Science Foundation of Jiangxi Province (20202BABL212011)

Biography: YANG Yu (1995-), male, PhD candidate. Research fields focus on applications of WGM resonator. E-mail: yangyu09@mail.ustc.edu.cn

\*Corresponding author: E-mail: kywang@ustc.edu.cn

## Introduction

The whispering gallery mode (WGM) resonator can confine the light in a cavity by total internal reflections around its inner surface, which can enhance the light power intensity in a very small mode volume and store the energy for a long time, in another word it means high  $Q$  factor or ultra-high  $Q$  factor can be provided<sup>[1-4]</sup>. Such resonators have attracted great attention for decades, due to it provides an ideal platform to investigate linear applications or nonlinear effects between light and matter, such as resonator sensing applications, cavity optomechanical research, light storage, and cavity quantum dot investigation<sup>[5-8]</sup>.

Crystal WGM resonators have been demonstrated as an ideal platform for nonlinear effects research<sup>[9]</sup>. It can be fabricated easily with the chemical mechanical polishing method, which has been investigated by Maleki and ultra-high  $Q$  factor can exceed in the order of  $10^9$ <sup>[10]</sup>. This ultra-high  $Q$  ensures a long photo lifetime and incredibly enhance the nonlinear effects. This is the reason why over the past two decades, applications into the mid-infrared and ultraviolet frequency ranges based on crystal WGM resonators have attracted so many optical researchers<sup>[11-12]</sup>.

Stimulated Brillouin scattering is the process that a pump photon interacts with lattice oscillation and is scattered into a Stokes photo and an acoustical photo<sup>[13]</sup>. During the SBS process, the pump wave is scattered into a Brillouin wave by the acoustic wave, and the effect of the acoustic wave is reinforced by the beating between the two optical waves through the electrostriction effect. Thus, SBS requires strict phase-matching conditions, considering both photo and phonon modes<sup>[14]</sup>. In the SBS process, it can generate two types of SBS, namely backward and forward scattering, due to the acoustic wave travel through different directions (Clockwise and Count-Clockwise). The schematic description of SBS process in WGM resonator is shown in Fig. 1. Stokes light can be amplified when it resonates with a resonance frequency in WGM resonators since the SBS is a coherent process. Due to the SBS threshold power is proportional to the mode volume and inversely proportional to the square of the  $Q$  factor, it can be easily generated at a low input power in WGM resonators which have high or ultra-high  $Q$  factor and a small mode volume.

SBS process can act as an ideal platform to investigate ultra-narrow linewidth lasers and ultra-sensitive gyroscopes since it has the advantage to combine the high signal level and low noise<sup>[15-17]</sup>. However, there is a limitation to achieve SBS in a single WGM resonator that the frequency of two optical modes must separate exactly to match the Brillouin frequency shift. Up to date, there are usually two methods to satisfy this condition. One is to precisely control the FSR in a large scale resonator, which is usually not an easy task for fabrication procedure. The other is to use different transverse modes in a resonator for the Stokes and the pump, which is hard to choose different modes when using prism or inclination fi-

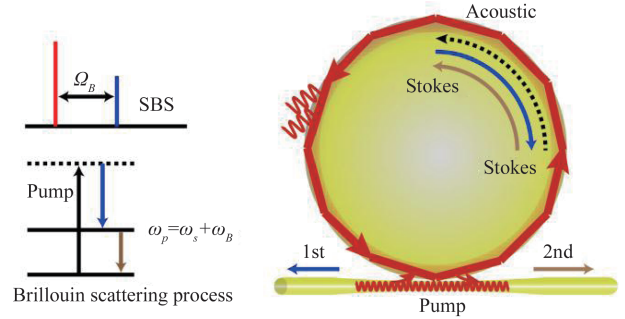


Fig. 1 The schematic description of SBS process in WGM resonator

图1 WGM谐振腔中的受激布里渊散射过程示意图

ber coupling methods<sup>[18-19]</sup>.

In this article, we present the observation results of the cascaded SBS in a  $\text{CaF}_2$  WGM resonator with an mm-sized 12.6 mm diameter and ultra-high  $Q$  factor  $1.16 \times 10^8$ . To lower the resonator fabrication difficulties to precisely control the FSR, we choose to employ different transverse modes to match the Brillouin frequency shift by using different positions of the optical tapered fiber to select different modes when coupling light into the resonator. During the experimental procedure, we found that the SBS stable state affected seriously by the fluctuation of the environment. To solve this problem, we devised a stable packaged platform for packaging the  $\text{CaF}_2$  WGM resonator and the tapered fiber. After packaging, the unstable problem can be perfectly solved and the packaged device can be used out of the laboratory. The result of the cascaded SBS and our packaged platform can be used in further investigation of SBS based resonator gyroscopes and SBS based lasers, which can significantly enhance the stability and sensitivity benefited from Brillouin nonlinear effect.

## 1 Experimental setup and packaged platform

The  $\text{CaF}_2$  crystal WGM resonator used in this experiment was fabricated through the chemical mechanical polishing method instead of the wet etching method mentioned in the literature, which ensures the resonator acquiring ultra-high  $Q$  factor and large scale<sup>[20-21]</sup>. The  $\text{CaF}_2$  resonator with an initial 15 mm diameter and 0.5 mm thickness was firstly mounted on an air rotation spindle, then the rough polishing procedure was used to get the initial circle shape, at last, the fine grinding procedure was adopted to acquire the ultra-smooth surface. During the procedure, the diamond abrasive paste and diamond water-based suspension was used as the polishing material. The ultra-high  $Q$  factor in a WGM resonator usually requires the root mean square (RMS) of the optically smooth surface to the sub-nanometer level, which can be measured by the white light interferometer.

The experimental setup about the generation of SBS is depicted in Fig. 2. It contains a tunable laser in a 1550 nm band, a function generator, a polarization controller, a three-dimensional coupling platform, a photo-

detector (PD), a spectrometer, and high-resolution digital oscilloscope. The tunable laser (New focus TLB 6728) was derived by a function generator. The laser beam polarization was adjusted by a polarization controller, then through into the tapered fiber and coupling into the micro-disk resonator. The transmission light was separated into two light beams, and one sent to an Optical spectrum analyzer (Yokogawa AQ6370D), the other sent to a photodetector where the transmission light transferred to an electrical signal. Finally, the electrical signal was recorded by a high-resolution digital oscilloscope (Keysight Infiniium MSOS604A).

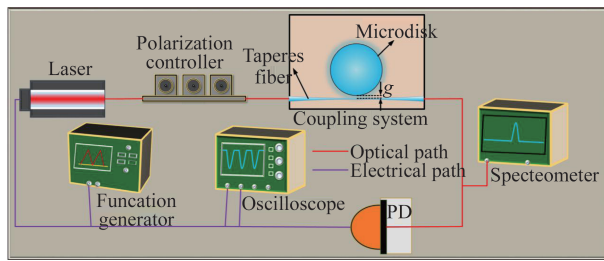


Fig. 2 The scheme of the experimental setup  
图2 实验系统结构框图

To solve the unstable problem, we designed a packaging platform which can package the CaF<sub>2</sub> resonator and the tapered fiber in an N<sub>2</sub> atmosphere. The packaging platform not only can protect the resonator and waveguide disturbed by the environmental fluctuation, but also ensure the coupling state adjustment. This is important for the further integrated SBS laser investigation. Figure 3 is the actual package platform with the resonator and a tapered fiber.

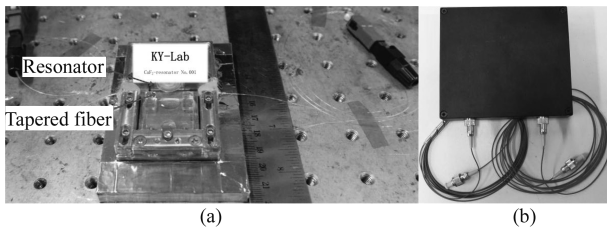


Fig. 3 (a) The packaged resonator and the waveguide, (b) the packaged resonator sealed in a box with two fiber connectors  
图3 (a)封装后的谐振腔与波导实物, (b)封装后谐振腔装入带两个光纤接头的密封盒中

## 2 Characteristics of the resonator

The WGM resonator has an attractive property that is their ability to confine the light into a small volume for a long time. This means the light photon has enough time to interact with the cavity matter. Usually, one method to calculate the  $Q$  factor of the WGM resonator is measuring the linewidth of the half maximum of the cavity mode at the condition of the weakly damped oscillator. The other is the ring-down spectroscopy. The former method is based on the formation  $Q \approx v/\Delta v$ , which consists of the linewidth of resonance  $\Delta v$  and the resonance frequency

$v$ . The  $Q$  factor measured using the former method is an approximate result which is usually half of the actual value. The later method to measure the  $Q$  factor is through measuring the photo lifetime  $\tau$  of resonance through the cavity ring-down since  $Q = 2\pi v\tau$ . It is more accurate than the former method, but it should be at the critical coupling condition which requires the more accurately adjust moving station and measure equipment. Take the deep consideration based on our measurement platform, we employ the former method to acquire the  $Q$  factor of our fabricated micro-disk CaF<sub>2</sub> resonator.

Figure 4(a) is the actual CaF<sub>2</sub> micro-disk resonator fabricated through our laboratory designed fabricating equipment<sup>[22]</sup>. The resonator has a 12.6 mm diameter after the polishing procedures and with a 0.1 mm rim thickness under the approximately 'V' shape condition. Figure 4(b) is the simulation result of the intrinsic mode in COMSOL software, which shows the electric field component distribution. Figure 4(c) is the sweeping power transmission spectrum between 1550 nm to 1550.2 nm. Figure 4(d) is the zoom in on a selected resonance mode from which the measured ultra-high  $Q$  factor is  $1.16 \times 10^8$ , which is based on the linewidth method. The calculation method based on the following equation,

$$Q \approx \lambda_0 / \Delta \lambda \quad (1)$$

where,  $\lambda_0$  is the central wavelength of the resonance,  $\Delta \lambda$  is the wavelength width of full width at half height. These two parameters can be calculated from the Lorentz fitting result of the resonance which is indicated by the red line in Fig. 4(d).

The Brillouin frequency shift is determined by the following equation<sup>[19]</sup>,

$$v_B = 2nv_a/\lambda \quad (2)$$

where the  $v_B$  is the Brillouin frequency shift,  $n$  is the refractive index,  $v_a$  is the speed of the acoustic wave and the  $\lambda$  is the wavelength of the light wave. Through the equation (2), we get the Brillouin frequency shift  $\Omega_B = 12.1$  GHz in our CaF<sub>2</sub> resonator at 1550 nm wavelength, which matches with literature<sup>[21]</sup>.

The SBS can appear as long as the pump power over the Brillouin threshold at the phase-matching condition. The threshold power is given by<sup>[23]</sup>,

$$P_{th} = \frac{\pi^3 n^2 V_m}{Bg_B \lambda_p \lambda_B Q_p Q_B} \quad (3)$$

where the  $n = 1.33$  is the refractive index of CaF<sub>2</sub> at 1.55  $\mu\text{m}$  wavelength,  $V_m = 12.6 \times 10^{-6} \text{cm}^3$  is the effective mode volume.  $B$  is the mode overlap which is close to 1 when the FSR is close to the Brillouin frequency shift.  $g_B = 2.8 \times 10^{-9} \text{cm/W}$  is the Brillouin gain of CaF<sub>2</sub>.  $Q_p = Q_B = 1.16 \times 10^8$ ,  $\lambda_p = \lambda_B = 1.55 \mu\text{m}$  are the  $Q$  factor and the wavelength of the pump and Brillouin lights, respectively. Based on these parameters, we obtained the  $P_{th} = 0.243 \text{mW}$  theoretical for our CaF<sub>2</sub> resonator.

## 3 Experimental results of SBS

WGM resonators with ultra-high  $Q$  factors are suitable for lower the SBS threshold power. But the SBS is usually realized in the fiber ring resonators, as they can

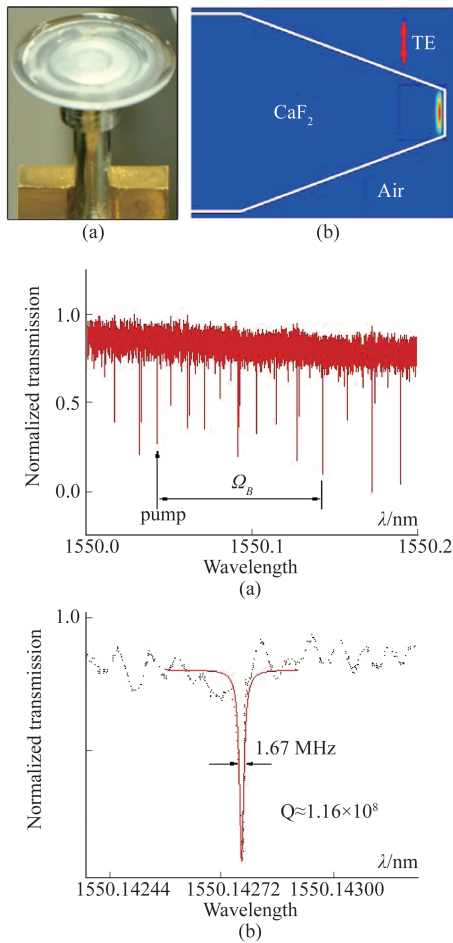


Fig. 4 (a)  $\text{CaF}_2$  resonator with 12.6 mm diameter and 0.1 mm rim thickness, (b) simulation result of the eigenmode distribution, (c) transmission spectrum contains multi-mode resonance, (d) calculating the quality factor based on a selected resonance  
图4 (a)  $\text{CaF}_2$  谐振腔实物, 直径 12.6 mm, 边缘厚度 0.1 mm, (b) 仿真的谐振腔本征模式分布结果, (c) 包含多个模式的传输谐振谱, (d) 拟合计算的谐振腔品质因子

easily have an FSR which is smaller than the SBS gain bandwidth to satisfy the double resonance condition, which means the pump and the scattered Stokes light frequency perfectly match the resonator resonance frequency in one FSR. The SBS typically has a bandwidth of tens of MHz and a frequency shift of the order of a few GHz. The calcium fluoride which we used for our resonator has an SBS bandwidth of 12 MHz. It is difficult to realize the Brillouin laser based on a single-mode ring resonator. This problem can be solved by the multimode structure of  $\text{CaF}_2$  WGM resonator, which can facilitate the SBS between the different WGM family.

To investigate the SBS in our  $\text{CaF}_2$  resonator and choose different WGM families, we imply the adiabatically tapered fiber with an approximate 1  $\mu\text{m}$  diameter twist as the waveguide, which was fabricated through the oxy-hydrogen flame heating method. During the tapered fiber fabrication procedure, the original 125  $\mu\text{m}$  diameter commercial optical fiber (Coning SFM-28) was gradually shrinking to 1  $\mu\text{m}$  twist, thus the tapered fiber has different propagation constant at different coupling positions,

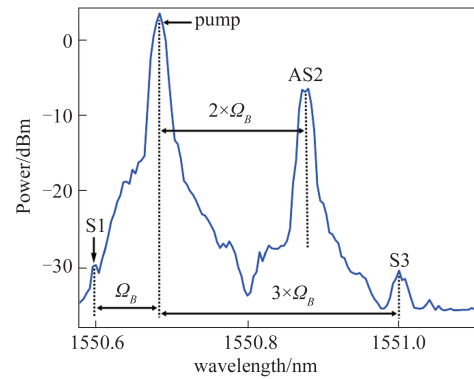


Fig. 5 the result of SBS contains three Brillouin lights  
图5 包含三阶布里渊激光的SBS实验结果

which ensure exciting the different mode families in our  $\text{CaF}_2$  resonator. Figure 5 shows the result of stimulated Brillouin lights in the forward direction which matches the Brillouin frequency shift  $\Omega_B = 12.1$  GHz or multi  $\Omega_B$ . The S1 and S3 represent the first order and third order Stokes light respectively, and the AS2 represents the second order anti-Stokes light.

During the procedure of increasing input power and detuning, the cascaded SBS occurred which up to the 5th Stokes in the forward direction. The corresponding result is depicted in Fig. 6. The position of each order Stokes light is indicated in the enlarged picture. However, it should be noted that the cascaded Brillouin lights have lower power. We believe that this is due to other nonlinear effects strongly happening around first and second Brillouin lights, which disperse the cascaded Brillouin light power. The nonlinear effects including stimulated Raman scattering and four-wave-mixing, which occur easily in WGM resonator as long as the pump power exceeds the threshold.

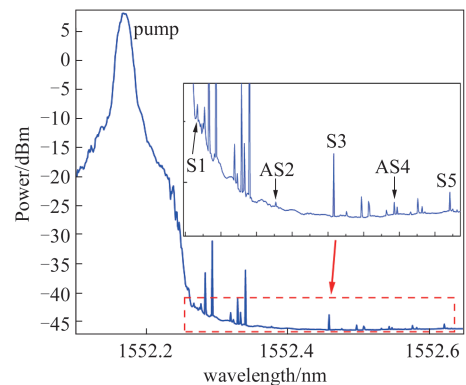


Fig. 6 The result of cascaded SBS up to fifth-order  
图6 达到5阶的级联SBS实验结果

## 4 Conclusions

In conclusion, we have reported the stimulated Brillouin scattering and the cascaded SBS in a millimeter size  $\text{CaF}_2$  WGM micro-disk resonator with ultra-high  $Q$  factor up to  $1.16 \times 10^8$ . Due to the large scale of the resonator, we observe multimode resonances between the res-

onator and the tapered fiber, which can perfectly match the SBS frequency shift. This eliminates the exact requirement of the diameter of a WGM resonator to generate stimulated Brillouin lights. To solve the problem of environment fluctuation, we designed a coupling platform for coupling light from tapered fiber to CaF<sub>2</sub> WGM resonator and a packaged box that can seal the coupling platform in N<sub>2</sub> atmosphere. Based on this packaged platform, we realized the cascaded Brillouin scattering with up to 5th Stokes (60.5 GHz frequency shift). This work and packaged resonator can further be used to investigate optical applications in infrared fields, such as packaged multi-wavelength Brillouin narrow linewidth laser and the packaged Brillouin gyroscope.

### Acknowledgment

This work was supported by the Fundamental Research Funds for the Central Universities (No. WK5290000001) and the Natural Science Foundation of Jiangxi Province (Nos. 20202BABL212011).

### References

- [1] Vahala K J. Optical microcavities [J]. *Nature*, 2003, **424**(6950): 839–46.
- [2] Yang S C, Wang Y, Sun H D. Advances and prospects for whispering gallery mode microcavities [J]. *Advanced Optical Materials*, 2015, **3**(9): 1136–62.
- [3] Xu W, Xu C X, Qin F F, *et al.* Whispering-gallery mode lasing from polymer microsphere for humidity sensing [J]. *Chin Opt Lett*, 2018, **16**(8): 081401.
- [4] Pan Z W, Zhang C F, Xie C F, *et al.* Resonator integrated optic gyro based on multilevel laser frequency lock-in technique [J]. *Chin Opt Lett*, 2018, **16**(4): 040601.
- [5] Dong C H, Shen Z, Zou C L, *et al.* Brillouin-scattering-induced transparency and non-reciprocal light storage [J]. *Nat Commun*, 2015, **6**(1): 6193.
- [6] Cheng M T, Ye G L, Zong W W, *et al.* Single photon scattering in a pair of waveguides coupled by a whispering-gallery resonator interacting with a semiconductor quantum dot [J]. *Chinese Physics Letters*, 2016, **33**(2): 024205.
- [7] Liu Y L, Wang C, Zhang J, *et al.* Cavity optomechanics: Manipulating photons and phonons towards the single-photon strong coupling [J]. *Chinese Physics B*, 2018, **27**(2): 024204.
- [8] Zhang Y N, Zhou T, Han B, *et al.* Optical bio-chemical sensors based on whispering gallery mode resonators [J]. *Nanoscale*, 2018, **10**(29): 13832–56.
- [9] Grudinin I S. Crystalline whispering gallery mode resonators for quantum and nonlinear optics [D]; California Institute of Technology, 2008.
- [10] Ilchenko V S, Savchenkov A A, Byrd J, *et al.* Crystal quartz optical whispering-gallery resonators [J]. *Opt Lett*, 2008, **33**(14): 1569–71.
- [11] Lin G P, Furst J, Strekalov D V, *et al.* High-Q UV whispering gallery mode resonators made of angle-cut BBO crystals [J]. *Optics Express*, 2012, **20**(19): 21372–8.
- [12] Lin G, Chembo Y K. On the dispersion management of fluorite whispering-gallery mode resonators for Kerr optical frequency comb generation in the telecom and mid-infrared range [J]. *Opt Express*, 2015, **23**(2): 1594–604.
- [13] Asano M, Takeuchi Y, Ozdemir S K, *et al.* Stimulated Brillouin scattering and Brillouin-coupled four-wave-mixing in a silica microbubble resonator [J]. *Opt Express*, 2016, **24**(11): 12082–92.
- [14] Sturman B, Breunig I. Brillouin lasing in whispering gallery microresonators [J]. *New Journal of Physics*, 2015, **17**(12): 125006.
- [15] Grudinin I S, Matsko A B, Maleki L. Brillouin lasing with a CaF<sub>2</sub> whispering gallery mode resonator [J]. *Phys Rev Lett*, 2009, **102**(4): 043902.
- [16] Diallo S, Lin G P, Martinenghi R, *et al.* Brillouin lasing in ultra-high-Q lithium fluoride disk resonators [J]. *IEEE Photonics Technology Letters*, 2016, **28**(9): 955–8.
- [17] Lu Q, Liu S, Wu X, *et al.* Stimulated Brillouin laser and frequency comb generation in high-Q microbubble resonators [J]. *Opt Lett*, 2016, **41**(8): 1736–9.
- [18] Guo C, Che K, Zhang P, *et al.* Low-threshold stimulated Brillouin scattering in high-Q whispering gallery mode tellurite microspheres [J]. *Opt Express*, 2015, **23**(25): 32261–6.
- [19] Lin G P, Chembo Y K. Opto-acoustic phenomena in whispering gallery mode resonators [J]. *International Journal of Optomechanics*, 2016, **10**(1): 32–9.
- [20] Long H, Yang W, Ying L Y, *et al.* Silica-based microcavity fabricated by wet etching [J]. *Chinese Physics B*, 2017, **26**(5): 054211.
- [21] Diallo S, Aubry J P, Chembo Y K. Effect of crystalline family and orientation on stimulated Brillouin scattering in whispering-gallery mode resonators [J]. *Opt Express*, 2017, **25**(24): 29934–45.
- [22] Wang M, Yang Y, Meng L, *et al.* Fabrication and packaging for high-Q CaF<sub>2</sub> crystalline resonators with modal modification [J]. *Chinese Optics Letters*, 2019, **17**(11): 111401.
- [23] Honda Y, Yoshiki W, Tetsumoto T, *et al.* Brillouin lasing in coupled silica toroid microcavities [J]. *Applied Physics Letters*, 2018, **112**(20): 201105.